

# A thermally stable heating mechanism for the intracluster medium: turbulence, magnetic fields and plasma instabilities

M. W. Kunz<sup>1\*</sup>, A. A. Schekochihin<sup>1</sup>, S. C. Cowley<sup>2,3</sup>, J. J. Binney<sup>1</sup> and J. S. Sanders<sup>4</sup>

<sup>1</sup> *Rudolf Peierls Centre for Theoretical Physics, University of Oxford, 1 Keble Road, Oxford, OX1 3NP, U. K.*

<sup>2</sup> *EURATOM/CCFE Fusion Association, Culham Science Centre, Abingdon, OX14 3DB, U. K.*

<sup>3</sup> *Blackett Laboratory, Imperial College, Prince Consort Road, London, SW7 2AZ, U. K.*

<sup>4</sup> *Institute of Astronomy, University of Cambridge, Madingley Road, Cambridge, CB3 0HA, U. K.*

Released 13/3/2010

## ABSTRACT

We consider the problem of self-regulated heating and cooling in galaxy clusters and the implications for cluster magnetic fields and turbulence. Viscous heating of a weakly collisional magnetised plasma is regulated by the pressure anisotropy with respect to the local direction of the magnetic field. The intracluster medium is a high-beta plasma, where pressure anisotropies caused by the turbulent stresses and the consequent local changes in the magnetic field will trigger very fast microscale instabilities. We argue that the net effect of these instabilities will be to pin the pressure anisotropies at a marginal level, controlled by the plasma beta parameter. This gives rise to local heating rates that turn out to be comparable to the radiative cooling rates. Furthermore, we show that a balance between this heating and Bremsstrahlung cooling is thermally stable, unlike the often conjectured balance between cooling and thermal conduction. Given a sufficient (and probably self-regulating) supply of turbulent power, this provides a physical mechanism for mitigating cooling flows and preventing cluster core collapse. For observed density and temperature profiles, the assumed balance of viscous heating and radiative cooling allows us to predict magnetic field strengths, turbulent velocities and turbulent scales as functions of distance from the centre. Specific predictions and comparisons with observations are given for two representative clusters: A1835 (cool-core) and Coma (non-cool-core). Our predictions can be further tested by future observations of cluster magnetic fields and turbulent velocities.

**Key words:** galaxies: clusters: intracluster medium — magnetic fields — instabilities — turbulence — diffusion — conduction

## 1 INTRODUCTION

Early X-ray observations of galaxy clusters and the intracluster medium (ICM) indicated radiative losses large enough to lead to cooling flows (see reviews by Sarazin 1986, 1988). Mass deposition rates  $\dot{M}_{\text{CF}}$  due to presumed cooling flows were estimated to be as much as  $\sim 10^3 \text{ M}_{\odot} \text{ yr}^{-1}$  in some clusters (Cowie & Binney 1977; Fabian & Nulsen 1977; Mathews & Bregman 1978). The cooling-flow model also predicts copious iron line emission from temperatures between  $10^6$  and  $10^7$  K. However, at the time there was little direct evidence for mass dropout in any spectral band other than X-rays (for a review, see Fabian 1994).

More recent high spectral resolution X-ray observations failed to detect the expected iron-line emission and constrained the central temperature to be  $\sim 1/3$  of the bulk cluster temperature (e.g. Peterson et al. 2001, 2003; Vikhlinin et al. 2005; Piffaretti et al. 2005; for a review, see Peterson & Fabian 2006). The spectroscopically determined mass deposition rates are  $\lesssim 0.1 \dot{M}_{\text{CF}}$  (e.g.

Voigt & Fabian 2004). This is despite the fact that the cooling time at  $r \lesssim 100$  kpc is less than a Hubble time in  $\gtrsim 70\%$  of clusters (e.g. Edge, Stewart & Fabian 1992; Peres et al. 1998; Sanderson, Ponman & O’ Sullivan 2006; Vikhlinin et al. 2006). This discrepancy is the so-called ‘cooling flow problem.’

Some heating source must therefore be balancing radiative cooling in the ‘cool-core’ clusters. A wide variety of heating and heat transport mechanisms have been considered, including thermal energy from the outer regions of the cluster being transported to the central cooling gas by conduction<sup>1</sup>; energy in jets, bubbles, cosmic rays, outflows and/or radiation from a central active galactic nucleus (AGN) either resulting in turbulent diffusion of

<sup>1</sup> Binney & Cowie (1981); Tucker & Rosner (1983); Bertschinger & Meiksen (1986); Gaetz (1989); Rosner & Tucker (1989); Narayan & Medvedev (2001); Voigt et al. (2002); Fabian, Voigt & Morris (2002); Zakamska & Narayan (2003); Kim & Narayan (2003b); Voigt & Fabian (2004); Balbus & Reynolds (2008); Bogdanović et al. (2009); Parrish, Quataert & Sharma (2009a,b)

\* E-mail: kunz@thphys.ox.ac.uk

heat<sup>2</sup> and/or being thermalised via dissipation of turbulent motions, sound waves and/or gravitational modes<sup>3</sup>; dynamical friction from galaxy wakes<sup>4</sup>; or some combination of these<sup>5</sup>. Much of recent work has focused on either thermal conduction, AGN heating, or both.

Thermal conduction alone cannot be the solution to the cooling flow problem across the full range of masses due to its steep temperature dependence (Voigt & Fabian 2004; Kaastra et al. 2004; Pope et al. 2006). Even in hot systems where conduction is potent, fine tuning of the suppression factor  $f$  (the fraction by which Spitzer conductivity is reduced due to, e.g., tangled magnetic field lines) is required (Bregman & David 1988). Moreover, if the thermal conduction has the same temperature dependence as the Spitzer conductivity (i.e. if  $f$  is constant) for a given ICM atmosphere, the resulting equilibria are thermally unstable (e.g. Bregman & David 1988; Soker 2003; Kim & Narayan 2003b; Guo & Oh 2008) — see further discussion in Sections 2.4 and 3.6.

More recently, however, there has been renewed interest in the possibility that thermal conduction may provide sufficient heating to stably counteract the effects of radiative cooling. This has gone hand-in-hand with a dramatic increase in our understanding of ‘dilute’ (i.e. only weakly collisional) plasmas, due to the appreciation that even very weak magnetic fields introduce an anisotropy into heat fluxes. One important consequence is that the criterion for convective instability changes to one of temperature, rather than entropy, increasing downwards (Balbus 2000, 2001). Quataert (2008) generalised Balbus’ (2000) analysis and found that a heat-flux buoyancy-driven instability (HBI) occurs for upwardly-increasing temperature profiles, so long as the magnetic field is not entirely horizontal (orthogonal to gravity). Balbus & Reynolds (2008) conjectured that the nonlinear HBI is self-regulating and drives a reverse convective thermal flux, both of which may mediate the stabilisation of cooling cores. Numerical simulations of the HBI have been performed by Parrish & Quataert (2008), Bogdanović et al. (2009) and Parrish, Quataert & Sharma (2009a) with applications to the ICM. It was discovered that the HBI acts to rapidly reorient field lines to insulate the core, undermining the role of thermal conduction and causing a cooling catastrophe to occur. Subsequent work has shown that a moderate amount of turbulent driving may help regulate the HBI and allow thermal channels to remain open, potentially stabilising the core against collapse (Sharma et al. 2009; Ruszkowski & Oh 2009; Parrish, Quataert & Sharma 2009b).

There are several reasons to believe that AGNs play an important role in regulating cooling. In many clusters, the

AGN energy output inferred from radio-emitting plasma outflows and cavities is similar to the X-ray cooling rate of the central gas (Fabian et al. 2000; Bîrzan et al. 2004; Dunn & Fabian 2006; McNamara & Nulsen 2007; Forman et al. 2007). Moreover,  $\gtrsim 70\%$  of cool-core clusters harbour radio sources at their centres, while  $\lesssim 25\%$  of clusters without cool cores are radio loud (Burns 1990), providing strong circumstantial evidence for a connection between the processes that fuel the radio emission (such as AGNs) and the X-ray emission from the cooling gas. Models of self-regulated heating from AGN have been constructed (e.g. Ciotti & Ostriker 2001; Ruszkowski & Begelman 2002; Brighenti & Mathews 2003; Kaiser & Binney 2003; Omma & Binney 2004; Hoeft & Brüggen 2004; Guo & Oh 2008; Brüggen & Scannapieco 2009) in which AGN activity is triggered by cooling-induced gas accretion toward cluster centres, increasing AGN heating and halting the collapse. Episodic outflows from AGN are thought not only to quench cooling and condensation in clusters, but also to limit the maximum luminosity of galaxies and regulate the growth of black holes at their centres (Binney 2005).

While AGN activity is fundamentally linked with the observed presence of radio bubbles and/or X-ray cavities (e.g. Bîrzan et al. 2004; Dunn & Fabian 2006), it is currently unclear how the AGN energy is actually thermalised (e.g. see the introduction of Voit & Donahue 2005 for a review of possibilities). This question can only be answered once knowledge of the effective viscosity of the ICM is acquired. The ICM hosts subsonic turbulence and dynamically-significant magnetic fields, both of which should affect the viscosity of the ICM (see review by Schekochihin & Cowley 2006). In particular, the presence of a magnetic field alters the form of the viscosity when the ratio of the ion cyclotron and collision frequencies is much greater than unity (Braginskii 1965), a condition trivially satisfied in galaxy clusters. As a result, the transport properties of the ICM become strongly dependent on both the geometry and strength of the magnetic field, as well as on microscale plasma instabilities that are likely to occur ubiquitously in the ICM (e.g. firehose, mirror; Schekochihin et al. 2005; Lyutikov 2007; Schekochihin et al. 2008, 2010; Rosin et al. 2010).

In this paper, we investigate the effect these plasma effects have on the large-scale transport properties of the ICM. Specifically, we argue that parallel viscous heating, due to the anisotropic damping of turbulent motions, is regulated by the saturation of microscale plasma instabilities (e.g., firehose, mirror) and can balance radiative cooling in the cool cores of galaxy clusters in such a way as to ensure thermal stability (Section 2). Given observed densities and temperatures, this balance implies specific values for central magnetic field strengths and radial profiles of the rms magnetic field that are in good agreement with current observational estimates and that lend themselves to testing by future observations (Section 3). We also show that, under the reasonable assumption that turbulent kinetic and magnetic energies are comparable to one another, cluster profiles for the turbulent velocity and the outer scale of turbulent motions may be derived. The specific case of A1835 is considered as a typical example in Section 3.4. Since the fundamental plasma-physical processes we appeal to are in principle universal in both cool-core and non-cool-core (i.e. unrelaxed) clusters, we also calculate in Section 3.5 the magnetic field strengths, turbulent velocities and turbulent lengthscales for the Coma cluster. They turn out to be in good agreement with current observational estimates. Thermal conduction and the robustness of our results with respect to it are briefly discussed in Section

<sup>2</sup> Deiss & Just (1996); Cho et al. (2003); Kim & Narayan (2003a); Voigt & Fabian (2004)

<sup>3</sup> Loewenstein & Fabian (1990); Binney & Tabor (1995); Ciotti & Ostriker (2001); Brüggen & Kaiser (2002); Omma & Binney (2004); Ruszkowski, Brüggen & Begelman (2004a,b); Churazov et al. (2004); Chandran (2004); Voit & Donahue (2005); Fabian et al. (2005); Brüggen, Ruszkowski & Hallman (2005); Chandran (2005); Fujita (2005); Donahue et al. (2006); Mathews, Faltenbacher & Brighenti (2006); Nusser, Silk & Babul (2006); Ciotti & Ostriker (2007); Chandran & Raseria (2007); McCarthy et al. (2008); Sijacki et al. (2008); Brüggen & Scannapieco (2009)

<sup>4</sup> Schipper (1974); Lea & De Young (1976); Rephaeli & Salpeter (1980); Miller (1986); Just et al. (1990); El-Zant, Kim & Kamionkowski (2004); Kim, El-Zant & Kamionkowski (2005); Dekel & Birnboim (2008)

<sup>5</sup> Ruszkowski & Begelman (2002); Brighenti & Mathews (2003); Brüggen (2003); Dennis & Chandran (2005); Fujita & Suzuki (2005); Pope et al. (2006); Conroy & Ostriker (2008); Guo & Oh (2008); Guo, Oh & Ruszkowski (2008)

3.6. In Section 4, we close with a discussion of our results and their limitations.

## 2 COOLING AND HEATING OF THE ICM

### 2.1 Radiative cooling

We follow Tozzi & Norman (2001) in approximating the radiative cooling rate (per unit volume) of the ICM (as determined by Sutherland & Dopita 1993) by

$$Q^- = n_i n_e \Lambda(T), \quad (1)$$

where the cooling function is

$$\Lambda(T) = 10^{-23} \text{ erg s}^{-1} \text{ cm}^3 \times \left[ C_1 \left( \frac{T}{1 \text{ keV}} \right)^{-1.7} + C_2 \left( \frac{T}{1 \text{ keV}} \right)^{0.5} + C_3 \right]. \quad (2)$$

Our notation is standard:  $n_i$  ( $n_e$ ) is the number density of ions (electrons) and  $T$  is the temperature (in energy units). We also define, for future use, the total number density  $n = n_i + n_e$ . The numerical constants  $C_1 = 0.086$ ,  $C_2 = 0.58$  and  $C_3 = 0.63$  are selected to correspond to an average metallicity  $Z = 0.3 Z_\odot$ , for which the mean mass per particle is  $\mu = 0.597 m_p$ , the mean mass per electron is  $\mu_e = \mu(n/n_e) = 1.150 m_p$  and  $n_i = 0.927 n_e$  (Sutherland & Dopita 1993). The cooling function is dominated by Bremsstrahlung above  $T \sim 1$  keV and by metal lines below  $T \sim 1$  keV.

Since the temperature equilibration time between ions and electrons  $t_{i-e,eq} \sim 10$  kyr near the centres and  $\sim 1$  Myr near the temperature maximum of cool-core clusters, which is smaller than all other timescales that will be relevant to us (see Section 3.6), we assume  $T_i = T_e = T$ . Even in unrelaxed clusters like Coma, where the temperature is relatively high ( $T \simeq 8.2$  keV; Arnaud et al. 2001) and the electron density is relatively low ( $n_e \simeq 3 \times 10^{-3} - 4 \times 10^{-5} \text{ cm}^{-3}$ ; see Section 3.5),  $t_{i-e,eq} \simeq 2 - 170$  Myr.

Normalised to conditions representative of the centres of cool-core clusters, the *radiative cooling rate* (per unit volume) is

$$Q^- \simeq 1.4 \times 10^{-25} \left( \frac{n_e}{0.1 \text{ cm}^{-3}} \right)^2 \left( \frac{T}{2 \text{ keV}} \right)^{1/2} \text{ erg s}^{-1} \text{ cm}^{-3} \quad (3)$$

in the Bremsstrahlung regime ( $T \gtrsim 1$  keV).

### 2.2 Parallel viscous heating

There is a rapidly growing body of observational evidence for the presence of appreciable magnetic fields in the ICM (for a review, see Carilli & Taylor 2002). Randomly tangled magnetic fields with strength  $B \sim 1 - 10 \mu\text{G}$  and characteristic scale  $\sim 1 - 10$  kpc are consistently found, with fields in the cool cores of cooling-flow clusters somewhat stronger than elsewhere (e.g. Murgia et al. 2004; Pollack, Taylor & Allen 2005; Vogt & Enßlin 2003, 2005; Kuchar & Enßlin 2009).

The presence of a magnetic field alters the form of the thermal pressure when  $\Omega_i/\nu_{ii} \gg 1$ , where  $\Omega_i (= eB/m_i c)$  is the ion cyclotron frequency and  $\nu_{ii} [= 4\sqrt{\pi} n_i \lambda_{ii} e^4 / 3 m_i^{1/2} T^{3/2}]$  is the ion-ion collision frequency;  $\lambda_{ii}$  is the ion-ion Coulomb logarithm (Braginskii 1965). This is certainly the case in the cool cores of galaxy clusters, where typical values of the electron density  $n_e$ , temperature  $T$  and magnetic field strength  $B$  imply

$$\frac{\Omega_i}{\nu_{ii}} = 5.8 \times 10^{10} \left( \frac{B}{10 \mu\text{G}} \right) \left( \frac{n_e}{0.1 \text{ cm}^{-3}} \right)^{-1} \left( \frac{T}{2 \text{ keV}} \right)^{3/2}. \quad (4)$$

As a result, thermal pressure becomes strongly anisotropic with respect to the local magnetic field direction  $\mathbf{b}$ :

$$\mathbf{P} = p_\perp (\mathbf{I} - \mathbf{b}\mathbf{b}) + p_\parallel \mathbf{b}\mathbf{b} \equiv p \mathbf{I} + \boldsymbol{\sigma}, \quad (5)$$

where  $p_\perp$  ( $p_\parallel$ ) is the thermal pressure perpendicular (parallel) to the local magnetic field,  $p = (2/3)p_\perp + (1/3)p_\parallel$  is the total thermal pressure,  $\mathbf{I}$  is the unit dyadic and we have defined the collisional viscous stress tensor

$$\boldsymbol{\sigma} = - \left( \mathbf{b}\mathbf{b} - \frac{1}{3} \mathbf{I} \right) (p_\perp - p_\parallel). \quad (6)$$

In the Braginskii (i.e. collisional) limit, appropriate for the large-scale motions in the ICM since any dynamical timescale is  $\gg \nu_{ii}^{-1} \gg \Omega_i^{-1}$ , the ion contribution to the viscous stress dominates that of the electrons by a factor proportional to  $(m_i/m_e)^{1/2}$ . Thus, in what follows we neglect the electron contribution to the viscous stress.

The viscous stress tensor appears both in the momentum equation,

$$m_i n_i \frac{d\mathbf{u}}{dt} = -\nabla \cdot \left[ \left( p_i + p_e + \frac{B^2}{8\pi} \right) \mathbf{I} - \frac{\mathbf{B}\mathbf{B}}{4\pi} + \boldsymbol{\sigma}_i \right] + m_i n_i \mathbf{g}, \quad (7)$$

as a form of momentum transport, and in the energy equation,

$$\frac{3}{2} n \frac{dT}{dt} = -nT \nabla \cdot \mathbf{u} - \boldsymbol{\sigma}_i : \nabla \mathbf{u} - \nabla \cdot \mathbf{q}_e - n_i n_e \Lambda, \quad (8)$$

as a form of heating. In these two equations,  $\mathbf{g}$  is the gravitational acceleration,  $n = n_i + n_e$  is the total number density,  $\mathbf{q}_e$  is the electron collisional heat flux and  $d/dt \equiv \partial/\partial t + \mathbf{u} \cdot \nabla$  is the convective derivative. We assume an ideal gas equation of state, so that  $p = nT$  (both for each species and for the two combined because  $T_i = T_e = T$ ). The electron contribution to the collisional heat flux dominates that of the ions by a factor of  $(m_i/m_e)^{1/2}$  (Braginskii 1965).

Differences between the perpendicular and parallel pressures in a magnetised plasma are due to the conservation of the first adiabatic invariant for each particle,  $\mu = mv_\perp^2/2B$  (on time scales  $\gg \Omega_i^{-1}$ ). Therefore, any change in the field strength must be accompanied by a corresponding change in the perpendicular pressure,  $p_\perp/B \sim \text{const}$ . In a turbulent plasma (such as the ICM), time-dependent fluctuations in the magnetic field strength are inevitable. Accordingly, a patchwork of regions of positive or negative pressure anisotropy will be set up corresponding to locally increasing or decreasing magnetic field strength. If the pressure anisotropy  $|p_\perp - p_\parallel| \gtrsim B^2/4\pi$ , firehose and mirror instabilities are triggered at spatial and temporal microscales (Schekochihin et al. 2005, and references therein).<sup>6</sup> Equations (7) and (8) break down at these scales, and the perpendicular and parallel pressures must be determined by a kinetic calculation (e.g. Schekochihin et al. 2010; Rosin et al. 2010).

It is usually the case that the pressure anisotropy — and thus the viscous stress — is regulated by the nonlinear evolution of these microscale instabilities, which tend to pin the pressure anisotropy at marginal stability values (Shapiro & Shevchenko

<sup>6</sup> In this paper we use the terms ‘microscales’ and ‘microscopic’ to describe processes whose lengthscales are just above the ion Larmor radius and whose growth rates are just below the ion cyclotron frequency.

1964; Quest & Shapiro 1996; Matteini et al. 2006; Lyutikov 2007; Schekochihin et al. 2008; Istomin, Pokhotelov & Balikhin 2009; Rosin et al. 2010):

$$\Delta_i \equiv \frac{p_{\perp,i} - p_{\parallel,i}}{p_i} = \frac{2\xi}{\beta_i}, \quad (9)$$

where  $\xi = -1$  for the firehose instability or 0.5 for the mirror instability.<sup>7</sup> The plasma beta parameter

$$\beta_i \equiv \frac{8\pi n_i T}{B^2} \simeq 75 \left( \frac{B}{10 \mu\text{G}} \right)^{-2} \left( \frac{n_e}{0.1 \text{ cm}^{-3}} \right) \left( \frac{T}{2 \text{ keV}} \right) \quad (10)$$

is the ratio of the (ion) thermal and magnetic pressures, normalised to conditions representative of the deep interiors of cool-core clusters. The recent observation that magnetic fluctuations in the solar wind are bounded by the firehose and mirror stability thresholds strongly supports this expectation (Kasper, Lazarus & Gary 2002; Hellinger et al. 2006; Matteini et al. 2007; Bale et al. 2009).

With a prescription for calculating the ion pressure anisotropy in hand, we would now like to calculate the implied heating rate (per unit volume) due to parallel viscous dissipation of motions. From Equations (6) and (8), this rate is given by

$$Q^+ = -\sigma_i : \nabla \mathbf{u} = p_i \Delta_i \left( \mathbf{b}\mathbf{b} : \nabla \mathbf{u} - \frac{1}{3} \nabla \cdot \mathbf{u} \right). \quad (11)$$

We seek to write this equation solely in terms of the ion pressure anisotropy, and therefore we require an additional equation relating the rate of strain (the term in parentheses) to the ion pressure anisotropy. This is provided by Braginskii (1965):

$$\nu_{ii} \Delta_i = 2.9 \left( \mathbf{b}\mathbf{b} : \nabla \mathbf{u} - \frac{1}{3} \nabla \cdot \mathbf{u} \right). \quad (12)$$

This equation states that the rate of strain due to turbulent motions generates a pressure anisotropy that is relaxed on the ion-ion collision timescale. Using Equation (12) in Equation (11), it follows that

$$Q^+ = 0.35 p_i \nu_{ii} \Delta_i^2. \quad (13)$$

In other words, the ion pressure anisotropy is a source of free energy that is eventually converted into heat by collisions.

Imposing marginality to microscale instabilities<sup>8</sup>, Equation (13) becomes

<sup>7</sup> In a turbulent plasma, there will be regions of pressure anisotropy with both signs and so one might expect some average value of  $\xi^2$  between 0.25 and 1. See also Sharma et al. (2006) for further refinements of this modelling.

<sup>8</sup> There are two fundamental physical ways in which marginal stability to microscale instabilities can be maintained in a weakly collisional plasma. *Either* microstabilities give rise to some effective particle scattering mechanism that isotropises the pressure (Schekochihin & Cowley 2006; Sharma et al. 2006, 2007) *or* they modify on the average the structure and time evolution of the magnetic field (or, equivalently, of the rate of strain) so as to cancel the pressure anisotropy caused by the changing fields. While there is no complete microphysical theory, existing calculations of particular cases (Schekochihin et al. 2008; Califano et al. 2008; Istomin, Pokhotelov & Balikhin 2009; Rosin et al. 2010; Rincon, Schekochihin & Cowley 2010, in preparation) all suggest the latter scenario. In this work we will *assume* that this is what happens. We interpret the right-hand side of Equation (12) as including contributions to the turbulent rate of strain from both the microscopic and macroscopic motions. Under the assumption that the collision frequency is not modified by the instabilities, Equation (12), together with Equation (9), states that microscale fluctuations in the magnetic field adjust themselves in response to large-scale fluid motions in order to maintain and preserve marginality.

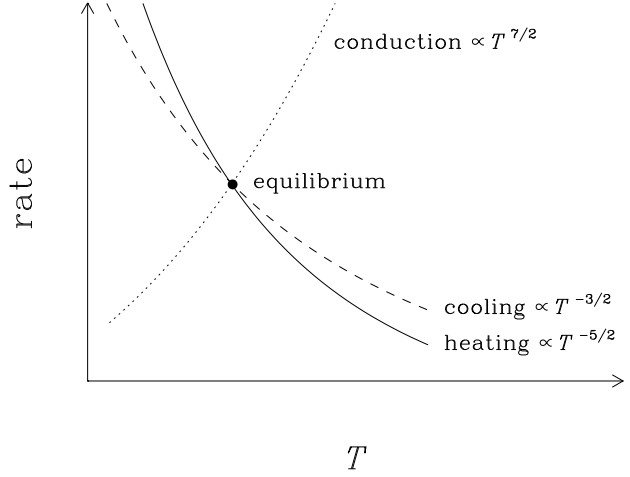


**Figure 1.** A sketch of the rates of parallel viscous heating (solid line) and radiative cooling (dashed line) versus temperature  $T$  at a fixed pressure. The thermal equilibrium point where heating balances cooling is denoted by a black dot. For a positive temperature perturbation from equilibrium, radiative cooling dominates over parallel viscous heating, whereas for a negative temperature perturbation from equilibrium, parallel viscous heating dominates over radiative cooling. Hence the equilibrium is stable to isobaric perturbations. By contrast, thermal balance between thermal conduction (dotted line) and radiative cooling is unstable.

$$Q^+ = 0.35 p_i \nu_{ii} \left( \frac{2\xi}{\beta_i} \right)^2 = 2.2 \times 10^{-3} \xi^2 B^4 \frac{\nu_{ii}}{p_i}. \quad (14)$$

Normalised to conditions representative of the centres of cool-core clusters, the *parallel viscous heating rate* (per unit volume) is

$$Q^+ = 10^{-25} \xi^2 \left( \frac{B}{10 \mu\text{G}} \right)^4 \left( \frac{T}{2 \text{ keV}} \right)^{-5/2} \text{ erg s}^{-1} \text{ cm}^{-3}. \quad (15)$$

Note the lack of an explicit dependence on density and also, remarkably, on either the amplitude or the rate of strain of the turbulence. However, the strong dependence on  $B$  does encode information about all of these. We stress that it is implicitly assumed that there is enough turbulence to maintain the pressure anisotropy at its stability threshold (eq. 9) — see further discussion of this point in Section 3.3 and at the end of Section 4.

### 2.3 Thermal balance and stability

The similarity between the coefficients in Equations (3) and (15) is striking and strongly suggests that *parallel viscous heating can offset radiative losses in the deep interiors of cluster cores*. However, it is not enough simply to find a heating source capable of balancing cooling. One must also ensure that the resulting equilibrium is thermally stable. This can be shown for our proposed heating mechanism as follows.

In Fig. 1, we show the rates of parallel viscous heating (solid line) and radiative cooling (dashed line) at fixed magnetic and thermal pressures as a function of temperature. The thermal equilibrium point where heating balances cooling is denoted by a black dot. The cooling rate (dashed line) scales as  $T^{-3/2}$  in the Bremsstrahlung regime, while the parallel viscous heating rate (solid line) scales as  $T^{-5/2}$ . Hence, if the temperature is perturbed downwards, the heating rate increases faster than the rate of radiative cooling, and net heating restores the temperature to its equilibrium.

librium value. On the other hand, if the temperature is perturbed upwards, the heating rate decreases faster than the rate of radiative cooling, and net cooling restores the temperature to its equilibrium value. In other words, *parallel viscosity, regulated by the growth of microscale instabilities, endows the large-scale plasma with a source of viscous heating that makes the plasma thermally stable.*

This is in stark contrast to a thermal balance between radiative cooling and thermal conduction (dotted line), whose heating rate scales as  $T^{7/2}$  at fixed thermal pressure. The resulting equilibrium is unstable, with an isobaric perturbation resulting in either an isothermal temperature profile (e.g. see fig. 7 of Parrish, Quataert & Sharma 2009a) or a cooling catastrophe. Thus, Spitzer conduction by itself cannot balance radiative cooling in a stable way (e.g. Bregman & David 1988; Soker 2003; Kim & Narayan 2003b; Binney 2004; Guo & Oh 2008).

The thermal stability argument for a balance between parallel viscous heating and radiative cooling may be refined by allowing for the possibility that the magnetic field strength is not fixed, but rather depends on density and temperature in some unknown way. (For the remainder of this Section we suppress the subscript  $i$  on  $n$  and  $\beta$  for economy of notation.) Again consider a thermal equilibrium, denoted by a subscript ‘0’, in which energy losses balance energy gains:

$$Q^-(n_0, T_0) = Q^+(T_0, B_0) \equiv Q_0, \quad (16)$$

where  $Q^-$  is given by Equation (1) and  $Q^+$  by Equation (14). Allow small perturbations to this equilibrium, denoted by  $\delta$ , which preserve a constant *total* pressure  $P$ :

$$\delta P = \delta p + \frac{B\delta B}{4\pi} + \frac{1}{3}(\delta p_\perp - \delta p_\parallel) = 0. \quad (17)$$

This effectively removes sound waves from the analysis (see eq. 7) and allows us to focus on non-propagating, subsonic (‘condensation’) modes (e.g. Field 1965). Further imposing marginality to microscale instabilities (eq. 9), Equation (17) becomes

$$\delta P = \delta p + \zeta \frac{B\delta B}{4\pi} = 0, \quad (18)$$

where  $\zeta \equiv 1 + 2\xi/3$ . Put simply, the pressure anisotropy modifies the magnetic pressure. Then the perturbed cooling and heating rates are, respectively,

$$\frac{\delta Q^-}{Q_0} \Big|_P = 2 \frac{\delta n}{n_0} + \frac{1}{2} \frac{\delta T}{T_0}, \quad (19)$$

$$\frac{\delta Q^+}{Q_0} \Big|_P = 4 \frac{\delta B}{B_0} - \frac{5}{2} \frac{\delta T}{T_0}. \quad (20)$$

If we define

$$\theta_T \equiv \frac{\partial \ln B}{\partial \ln T} \Big|_{n,0} \quad \text{and} \quad \theta_n \equiv \frac{\partial \ln B}{\partial \ln n} \Big|_{T,0}, \quad (21)$$

we find that the fractional perturbation in the density is related to the fractional perturbation in the temperature by

$$\frac{\delta n}{n_0} = -\frac{\delta T}{T_0} \left( \frac{1 + 2\zeta\theta_T/\beta_0}{1 + 2\zeta\theta_n/\beta_0} \right). \quad (22)$$

Note that this reduces to requiring a constant thermal pressure in the limit  $\beta_0 \gg 1$ . Substituting Equation (22) into Equations (19) and (20), we find

$$\frac{\delta Q^-}{Q_0} \Big|_P = +\frac{\delta T}{T_0} \left[ \frac{1}{2} - 2 \left( \frac{1 + 2\zeta\theta_T/\beta_0}{1 + 2\zeta\theta_n/\beta_0} \right) \right], \quad (23)$$

$$\frac{\delta Q^+}{Q_0} \Big|_P = -\frac{\delta T}{T_0} \left[ \frac{5}{2} - 4 \left( \frac{\theta_T - \theta_n}{1 + 2\zeta\theta_n/\beta_0} \right) \right]. \quad (24)$$

From this, it follows that the loss function (i.e. heat losses minus heat gains) is

$$\begin{aligned} \mathcal{L}(n, T, B) \Big|_P &\equiv Q^-(n, T, B) \Big|_P - Q^+(n, T, B) \Big|_P \\ &= Q_0 \frac{\delta T}{T_0} \left[ 1 - 4 \left( 1 + \frac{\zeta}{\beta_0} \right) \left( \frac{\theta_T - \theta_n}{1 + 2\zeta\theta_n/\beta_0} \right) \right]. \end{aligned} \quad (25)$$

Since  $\beta \gg 1$  in the ICM (see eq. 10),

$$\mathcal{L}(n, T, B) \Big|_P \simeq Q_0 \frac{\delta T}{T_0} \left[ 1 - 4(\theta_T - \theta_n) \right]. \quad (26)$$

To ensure thermal stability, the term in square brackets must be non-negative, so that the loss function has the same sign as  $\delta T$ . Then, by Equation (26),

$$\frac{\partial \ln B}{\partial \ln T} \Big|_n - \frac{\partial \ln B}{\partial \ln n} \Big|_T \leq \frac{1}{4} \quad (\text{for thermal stability}). \quad (27)$$

This inequality is marginally satisfied (by definition) if heating balances cooling. Unless the perturbed magnetic field is a strongly increasing function of temperature or the magnetic field increases with decreasing density, neither of which are particularly likely, the inequality (27) is satisfied and so the equilibrium is thermally stable.

### 3 IMPLICATIONS: CLUSTER EQUILIBRIUM PROFILES

Given the promise of parallel viscous heating simultaneously to balance radiative cooling and stabilise the centres of cool-core clusters, it is tempting to ascribe the entire temperature profile inside the cooling radius to a long-term balance between this form of heating and cooling. In this section, we investigate what this implies for magnetic field strengths, turbulent velocities and turbulent scales throughout cluster cores as a function of radius  $r$ .

#### 3.1 Magnetic fields

We assume that parallel viscous heating (eq. 15) due to turbulent dissipation balances radiative cooling (eq. 3) at all radii inside the cluster core:

$$Q^+ \simeq Q^-. \quad (28)$$

In the Bremsstrahlung regime, this implies

$$B \simeq 11 \xi^{-1/2} \left( \frac{n_e}{0.1 \text{ cm}^{-3}} \right)^{1/2} \left( \frac{T}{2 \text{ keV}} \right)^{3/4} \mu\text{G}. \quad (29)$$

Note that *the predicted magnetic field strength is a function of density and temperature*. It is common in both numerical modelling of clusters (e.g. Dolag et al. 2001) and in data analysis aiming to reconstruct magnetic field strengths and spectra (e.g. Murgia et al. 2004; Kuchar & Enßlin 2009) to assume an exclusive relationship between  $B$  and  $n_e$ . Our arguments suggest that these models may need to be generalised to accommodate the temperature dependence.

For typical electron densities ( $n_e \sim 0.01 - 0.1 \text{ cm}^{-3}$ ) and temperatures ( $T \sim 1 - 3 \text{ keV}$ ) at the centres of cool-core clusters, Equation (29) implies central magnetic fields  $\sim 1 - 10 \mu\text{G}$ , easily within observational constraints. For example, conditions near the

centre of the popular Hydra A cluster ( $n_e \simeq 0.07 \text{ cm}^{-3}$  and  $T \simeq 3 \text{ keV}$ ; David et al. 2001) imply a thermal-equilibrium magnetic field strength  $B \simeq 12 \xi^{-1/2} \mu\text{G}$ . Farther out around  $\simeq 30 \text{ kpc}$ , the observed electron density  $n_e \simeq 0.02 \text{ cm}^{-3}$  and temperature  $T \simeq 3.5 \text{ keV}$  imply  $B \simeq 7 \xi^{-1/2} \mu\text{G}$ . These are both in good agreement with magnetic field strength estimates in Hydra A from Faraday rotation maps (Vogt & Enßlin 2003, 2005). For another cluster A2199, popular among theorists (e.g. Parrish, Quataert & Sharma 2009a), a central density  $n_e \simeq 0.1 \text{ cm}^{-3}$  and central temperature  $T \simeq 2 \text{ keV}$  (Johnstone et al. 2002; H. Russell, private communication) imply  $B \simeq 11 \xi^{-1/2} \mu\text{G}$ .

### 3.2 Turbulent velocities

In order to estimate the turbulent velocities in the ICM, we assume that the large-scale kinetic and magnetic energies are in overall equipartition,

$$\frac{1}{2} m_i n_i U_{\text{rms}}^2 \simeq \frac{B^2}{8\pi}, \quad (30)$$

where  $U_{\text{rms}} \equiv \langle u^2 \rangle^{1/2}$  is the rms flow velocity. This is expected to be the case for a magnetic field amplified and brought to saturation by the fluctuation dynamo (e.g. Schekochihin & Cowley 2007, and references therein). Then the rms turbulent velocity is equal to the Alfvén speed and, using Equation (29),

$$U_{\text{rms}} \simeq 70 \xi^{-1/2} \left( \frac{T}{2 \text{ keV}} \right)^{3/4} \text{ km s}^{-1} \quad (31)$$

in the Bremsstrahlung regime. In other words, *relatively hotter (cooler) cores should therefore have larger (smaller) turbulent velocities*. The corresponding Mach number is

$$M \equiv \frac{U_{\text{rms}}}{c_s} = 0.18 \xi^{-1/2} \left( \frac{T}{2 \text{ keV}} \right)^{1/4}, \quad (32)$$

where  $c_s = (T/m_i)^{1/2}$  is the sound speed. Note the weak dependence of  $M$  on temperature. For  $T \simeq 1 - 10 \text{ keV}$ ,  $U_{\text{rms}}$  ranges from  $\simeq 44 \xi^{-1/2} \text{ km s}^{-1}$  to  $210 \xi^{-1/2} \text{ km s}^{-1}$ , so  $M$  ranges from  $\simeq 0.16 \xi^{-1/2}$  to  $0.24 \xi^{-1/2}$ . While the turbulent velocities are not yet measured directly, theoretical (e.g. Dennis & Chandran 2005; Enßlin & Vogt 2006; Subramanian, Shukurov & Haugen 2006; Iapichino & Niemeyer 2008), numerical (e.g. Norman & Bryan 1999; Ricker & Sarazin 2001; Sunyaev, Norman & Bryan 2003) and indirect observational (e.g. Schuecker et al. 2004; Churazov et al. 2004; Rebusco et al. 2005, 2006; Graham et al. 2006; Rebusco et al. 2008; Sanders et al. 2009) estimates suggest that the numbers we are predicting are reasonable.

We caution here that Equation (31) should be considered a lower limit on the actual turbulent velocity since  $U_{\text{rms}}$  is unlikely to be smaller, but could be larger, than the Alfvén speed. In magnetohydrodynamic numerical simulations, it is often larger by a factor of order unity (e.g. Schekochihin et al. 2004; Haugen, Brandenburg & Dobler 2004).

### 3.3 Turbulent scales

Implicit in the above discussion is the requirement that there be enough turbulent energy for the viscous heating rate mandated by the marginal stability condition (see eq. 14) to be maintained. We assume that throughout the cluster core all of the power from external stirring (see discussion in Section 4) accepted by the turbulence is locally dissipated and thermalised via parallel viscosity:

$$m_i n_i \frac{U_{\text{rms}}^2}{\tau_{\text{turb}}} \simeq Q^+, \quad (33)$$

where  $\tau_{\text{turb}}^{-1}$  is the effective rate at which energy is converted into turbulent motions. In conventional turbulence, this is equivalent to the eddy turnover timescale. In writing Equation (33), we have ignored the possibility that energy could cascade to collisionless scales via Alfvénic turbulence and heat the plasma via microphysical dissipation at the ion and electron Larmor scales (Schekochihin et al. 2009).

Equations (31) and (33) give

$$\tau_{\text{turb}} \simeq 2 \xi^{-1} \left( \frac{n_e}{0.1 \text{ cm}^{-3}} \right)^{-1} \left( \frac{T}{2 \text{ keV}} \right) \text{ Myr}. \quad (34)$$

We also define the turbulent outer lengthscale

$$\begin{aligned} L &\equiv \alpha U_{\text{rms}} \tau_{\text{turb}} \\ &\simeq 0.2 \alpha \xi^{-3/2} \left( \frac{n_e}{0.1 \text{ cm}^{-3}} \right)^{-1} \left( \frac{T}{2 \text{ keV}} \right)^{7/4} \text{ kpc}, \end{aligned} \quad (35)$$

where  $\alpha$  is some adjustable factor that encodes the efficiency of energy absorption (in conventional turbulence,  $\alpha \sim 1$ ). While we do not know *a priori* the values of  $\alpha$  or  $L$  individually, we can determine their ratio  $L/\alpha$  from Equation (35). We will see that this is in fact close to what the outer scale is generally expected to be, so  $\alpha \sim 1$  is probably a good estimate. In what follows we suppress  $\alpha$  in the definition of  $L$ .

A corollary of Equations (31) and (34) is that the turbulent diffusion coefficient is

$$\begin{aligned} \kappa_{\text{turb}} &\sim U_{\text{rms}}^2 \tau_{\text{turb}} \\ &\simeq 3 \times 10^{27} \xi^{-2} \left( \frac{n_e}{0.1 \text{ cm}^{-3}} \right)^{-1} \left( \frac{T}{2 \text{ keV}} \right)^{5/2} \text{ cm}^2 \text{ s}^{-1}. \end{aligned} \quad (36)$$

Interestingly,  $\kappa_{\text{turb}}$  has the same scaling as the Spitzer (1962) electron thermal diffusion coefficient (see Section 3.6).

### 3.4 Cool-core cluster profiles: A1835

Using Equations (29) – (36), profiles of  $B$ ,  $U_{\text{rms}}$ ,  $L$  and  $\kappa_{\text{turb}}$  may be calculated for any given cluster. Here we provide results for one particular cool-core cluster, A1835 (we have performed the same exercise for many other clusters, with similarly sensible outcomes). In Fig. 2 we give the observed (deprojected) electron number density  $n_e$ , observed (deprojected) temperature  $T$ , predicted magnetic field strength  $B$ , predicted rms outer-scale velocity  $U_{\text{rms}}$ , predicted turbulent outer scale  $L$  and predicted turbulent diffusion coefficient  $\kappa_{\text{turb}}$ . The density and temperature profiles are from Sanders et al. (2009). The data points for the predicted quantities use  $|\xi| = 0.75$ , but we also show upper and lower limits calculated by setting  $|\xi| = 0.5$  (dashed lines) and  $|\xi| = 1$  (dotted lines), respectively.

The predicted value for  $B$  near the centre of the core is  $\simeq 15 - 21 \mu\text{G}$ , decreasing to  $\simeq 5 - 7 \mu\text{G}$  at the outer core boundary. To our knowledge, observational estimates of the magnetic field strength in A1835 have not yet appeared in the literature. As a radio mini-halo has recently been detected in A1835 (Murgia et al. 2009), there is hope for a magnetic field measurement there, although this might be quite a difficult task for such a distant cluster. The predicted turbulent velocity dispersion  $U_{\text{rms}} \sim 70 - 270 \text{ km s}^{-1}$  throughout the core, attaining a value  $U_{\text{rms}} \simeq 114 - 162 \text{ km s}^{-1}$  at a radius of  $30 \text{ kpc}$ . This is within the  $182 \text{ km s}^{-1}$  upper limit obtained by Sanders et al. (2009) by measuring emission lines within

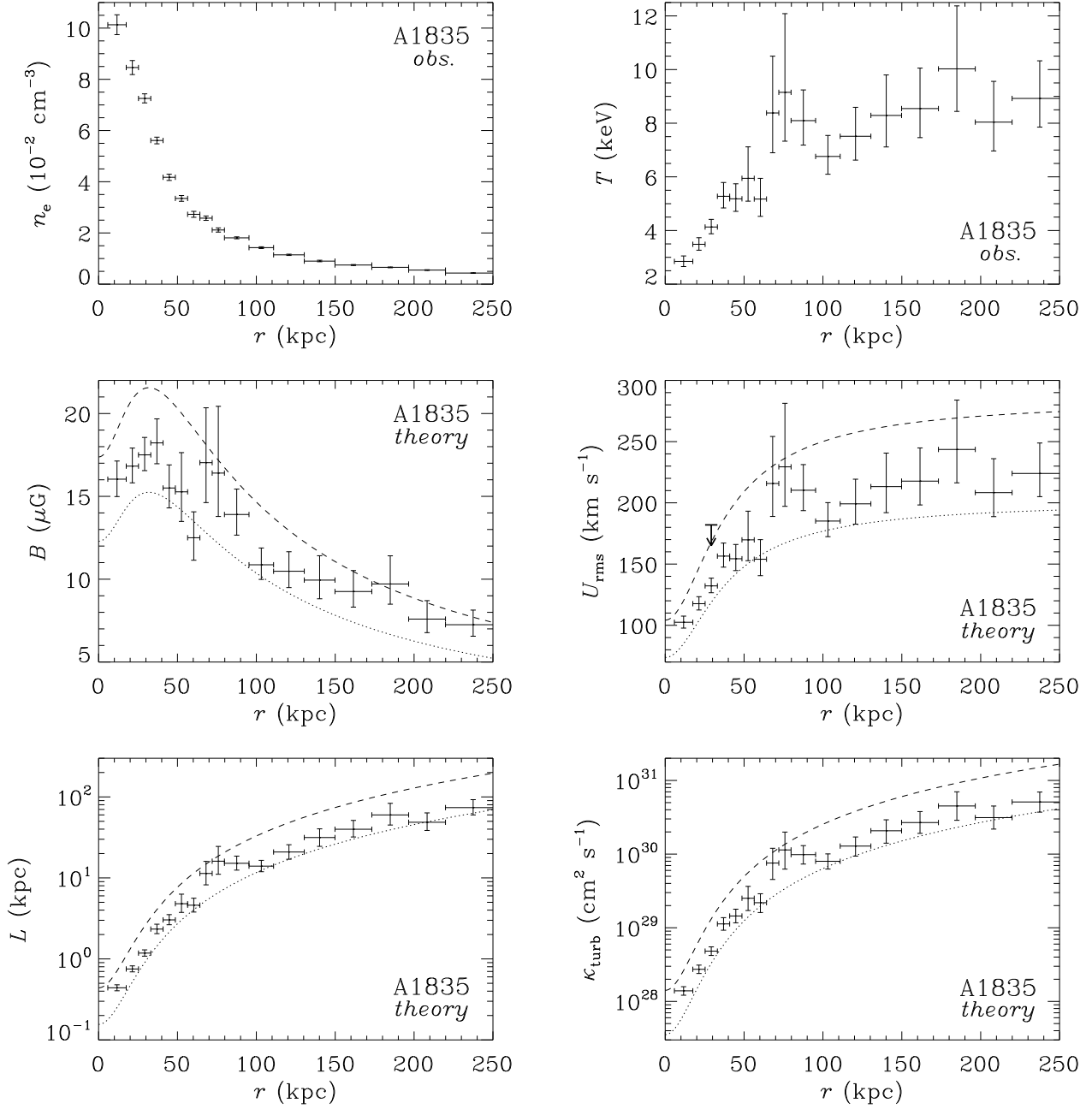


**Figure 2.** (Left to right, top to bottom) Profiles of the observed (deprojected) electron number density  $n_e$ , observed (deprojected) temperature  $T$ , predicted magnetic field strength  $B$ , predicted rms outer-scale velocity  $U_{\text{rms}}$ , predicted outer turbulent lengthscale  $L$  and predicted turbulent diffusion coefficient  $\kappa_{\text{turb}}$  for the cool-core cluster A1835. The predicted data points correspond to  $|\xi| = 0.75$ , halfway between the firehose instability threshold ( $|\xi| = 1$ ; dotted line) and the mirror instability threshold ( $|\xi| = 0.5$ ; dashed line). The line plots are derived from best-fitting analytic profiles to the electron number density and temperature (see footnote 9). The thick arrow on the plot of  $U_{\text{rms}}$  denotes the  $182 \text{ km s}^{-1}$  observationally-derived upper limit obtained by Sanders et al. (2009) at  $r \simeq 30 \text{ kpc}$ .

$r \simeq 30 \text{ kpc}$ , which is denoted on the plot by a thick arrow. A more conservative observational estimate of  $U_{\text{rms}} \lesssim 274 \text{ km s}^{-1}$  Sanders et al. (2009) was derived by treating the cluster as a point source and not applying any spatial smoothing. The predicted turbulent outer scale  $L \sim 0.2 - 0.7 \text{ kpc}$  near the centre of the core, increasing outwards to  $\sim 70 - 200 \text{ kpc}$  near the temperature maximum. The predicted diffusion coefficient  $\kappa_{\text{turb}}$  rises sharply from

$\sim 10^{28} \text{ cm}^2 \text{ s}^{-1}$  near the core centre to  $\sim 10^{31} \text{ cm}^2 \text{ s}^{-1}$  at the outer core boundary. Given the uncertainties discussed in Sections 3.2 and 3.3, it is encouraging that these values are comparable to the inferred diffusion coefficients  $\sim 10^{29} - 10^{30} \text{ cm}^2 \text{ s}^{-1}$  in a variety of observed clusters (Rebusco et al. 2005, 2006, 2008; David & Nulsen 2008).

### 3.5 Non-cool-core cluster profiles

The plasma microphysics responsible for parallel viscous heating is in no way unique to cool-core clusters. Since plenty of turbulence is expected to be present (coming from mergers, etc.), pressure anisotropies will develop and will presumably be maintained at a marginal level as described in Section 2.2. While heating and cooling times are quite long in such clusters and the situation can be quite time-dependent, we would nevertheless like to explore what the conjecture of an approximate local heating-cooling balance would imply, with the caveat that such a balance may in principle take a very long time to be established. We will see that such a balance appears to lead to quite reasonable predictions that seem to be borne out by observational data.

In isothermal clusters, Equations (29) – (35) imply that

$$B \propto n_e^{1/2}, \quad (37)$$

$$U_{\text{rms}} \simeq \text{const}, \quad (38)$$

$$\tau_{\text{turb}} \propto L \propto n_e^{-1}. \quad (39)$$

The scaling  $B \propto n_e^{1/2}$  in non-cool-core clusters has in fact already been observationally inferred for A2382 (Guidetti et al. 2008), Coma (Bonafede et al. 2010) and A665 (Vacca et al. 2010).

The central density  $n_e \simeq 5 \times 10^{-3} \text{ cm}^{-3}$  and temperature  $T \simeq 2.9 \text{ keV}$  in A2382 implies a thermal-equilibrium magnetic field strength  $B \simeq 3.1 \xi^{-1/2} \mu\text{G}$ , in excellent agreement with the  $\sim 3 \mu\text{G}$  estimate derived from rotation measure observations (Guidetti et al. 2008). For A2255,  $n_e \simeq 2 \times 10^{-3} \text{ cm}^{-3}$  (Feretti et al. 1997; Govoni et al. 2006) and  $T \simeq 3.5 \text{ keV}$  (Davis & White 1998, however, see Sakellou & Ponman 2006, who find temperature variations across A2255 from  $T \sim 5.5 - 8.5 \text{ keV}$ ), the thermal-equilibrium magnetic field strength  $B \simeq 2.2 \xi^{-1/2} \mu\text{G}$ . This compares favourably with the observational estimate  $B \sim 2.5 \mu\text{G}$  obtained by Govoni et al. (2006), who used  $B \propto n_e^{1/2}$  in their analysis.

Very recently there have been observational estimates of the magnetic field strength profile in the non-cool-core Coma cluster (Bonafede et al. 2010). It is of interest to see what the foregoing discussion implies for Coma. We model Coma as an isothermal cluster with temperature  $8.2 \text{ keV}$  (Arnaud et al. 2001) and with a ‘ $\beta$ -model’ (Cavaliere & Fusco-Femiano 1976) electron density profile

$$n_e = n_0 \left(1 + \frac{r^2}{r_c^2}\right)^{-3\beta/2} \quad (40)$$

with  $n_0 = 3.44 \times 10^{-3} \text{ cm}^{-3}$ ,  $r_c = 291 \text{ kpc}$  and  $\beta = 0.75$  (Bonafede et al. 2010). Then Equations (29) – (36) become

$$B \simeq 5.3 \xi^{-1/2} \left(1 + \frac{r^2}{r_c^2}\right)^{-9/16} \mu\text{G}, \quad (41)$$

$$U_{\text{rms}} \simeq 183 \xi^{-1/2} \text{ km s}^{-1}, \quad (42)$$

$$M \simeq 0.23 \xi^{-1/2}, \quad (43)$$

$$\tau_{\text{turb}} \simeq 278 \xi^{-1} \left(1 + \frac{r^2}{r_c^2}\right)^{9/8} \text{ Myr}, \quad (44)$$

$$L \simeq 52 \xi^{-3/2} \left(1 + \frac{r^2}{r_c^2}\right)^{9/8} \text{ kpc}, \quad (45)$$

$$\kappa_{\text{turb}} \simeq 3 \times 10^{30} \xi^{-2} \left(1 + \frac{r^2}{r_c^2}\right)^{9/8} \text{ cm}^2 \text{ s}^{-1}. \quad (46)$$

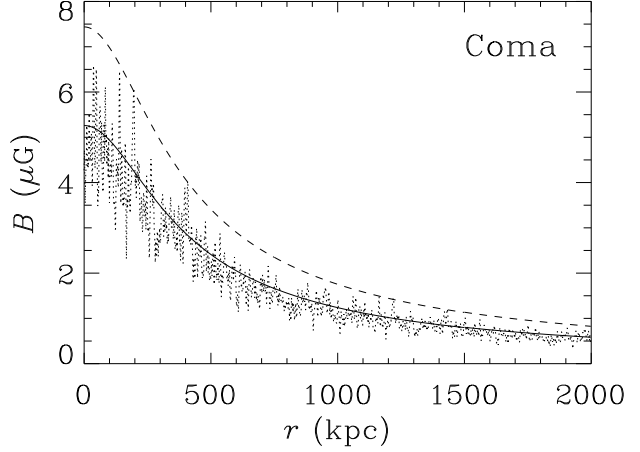


**Figure 3.** Profile of the predicted magnetic field strength  $B$  in the non-cool-core cluster Coma for  $|\xi| = 1$  (firehose instability threshold; solid line) and  $|\xi| = 0.5$  (mirror instability threshold; dashed line). The dotted line represents the observed magnetic field power spectrum fluctuations, as determined by Bonafede et al. (2010).

Observations of turbulence via pressure maps in the innermost  $r \simeq 215 \text{ kpc}$  of the Coma cluster (Schuecker et al. 2004) indicated that  $L \sim 100 \text{ kpc}$  there. Our predicted outer scale of the turbulence at  $r \simeq 215 \text{ kpc}$  is  $L \simeq 85 \xi^{-3/2} \text{ kpc}$ .

The predicted rms magnetic field profile (eq. 41) is shown in Fig. 3 for  $|\xi| = 1$  (firehose instability threshold; solid line) and  $|\xi| = 0.5$  (mirror instability threshold; dashed line). Overlaid are the observed power spectrum fluctuations from Bonafede et al. (2010), as determined by comparing the observed Faraday rotation measure with simulated rotation measure images and finding the best fit. The theory appears sensible despite all the uncertainties. It is encouraging that no fine-tuning of prefactors was required to obtain this result.

### 3.6 Postscript: thermal conduction

Bearing in mind that thermal conduction models routinely fail in the innermost regions of cool cluster cores (e.g. see Markevitch et al. 2003; Kaastra et al. 2004; Ghizzardi et al. 2004), it is important to note that parallel viscous heating should be especially important in these relatively cold ( $T \sim 1 \text{ keV}$ ) and strongly-magnetised ( $B \sim 10 \mu\text{G}$ ) regions. A balance between parallel viscous heating and radiative cooling, however, does contain the implicit assumption that the thermal conduction is relatively unimportant. This ought to be checked.

The Spitzer (1962) electron thermal diffusion coefficient is

$$\kappa_{\text{Sp}} \simeq 10^{29} \left(\frac{n_e}{0.1 \text{ cm}^{-3}}\right)^{-1} \left(\frac{T}{2 \text{ keV}}\right)^{5/2} \text{ cm}^2 \text{ s}^{-1}. \quad (47)$$

In tangled turbulent magnetic fields, the true thermal conductivity is expected to be  $\kappa = f \kappa_{\text{Sp}}$ , where  $f$  is the suppression factor, which is expected to range anywhere between  $\sim 10^{-3}$  and  $\sim 0.3$  (Tribble 1989; Tao 1995; Pistinner & Shaviv 1996; Chandran & Cowley 1998; Chandran et al. 1999; Narayan & Medvedev 2001; Gruzinov 2002; Cho et al. 2003). Note that the Spitzer diffusion coefficient has the same density and temperature scaling as the turbulent diffusion coefficient derived in Section 3.3. We see that for  $f \lesssim 0.03 \xi^{-2}$ , turbulent heat diffusion is likely to be at least as important as the collisional conductivity.



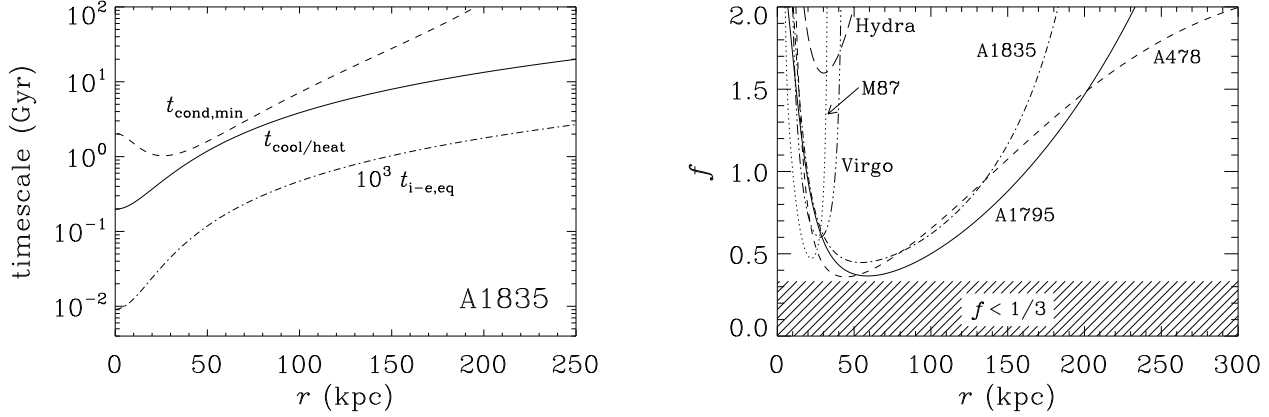


**Figure 4.** (a) The cooling/heating timescale  $t_{\text{cool/heat}}$  (solid line), ion-electron equilibration timescale  $t_{i-e,eq}$  (dash-dot line) and the shortest possible conduction timescale  $t_{\text{cond,min}}$  (dashed line) for A1835. (b) The Spitzer conduction suppression factor  $f \equiv \kappa/\kappa_{\text{Sp}}$  required for thermal conduction to balance radiative cooling as a function of radius for several different clusters. Only suppression factors  $f \lesssim 1/3$  (shaded region) are allowed in the presence of a tangled magnetic field. The line plots are derived from best-fitting analytic profiles to the electron number densities and temperatures (see footnote 9).

In Fig. 4a, we plot for A1835 the cooling/heating timescale

$$t_{\text{cool/heat}} = \frac{3}{2} \frac{nT}{Q^-} = 0.23 \left( \frac{n_e}{0.1 \text{ cm}^{-3}} \right)^{-1} \left( \frac{T}{2 \text{ keV}} \right)^{1/2} \text{ Gyr}, \quad (48)$$

the ion-electron temperature equilibration timescale

$$t_{i-e,eq} = 9.3 \left( \frac{n_e}{0.1 \text{ cm}^{-3}} \right)^{-1} \left( \frac{T}{2 \text{ keV}} \right)^{3/2} \text{ kyr}, \quad (49)$$

and the shortest possible conduction timescale

$$t_{\text{cond,min}} = \frac{3}{2} nT \left[ \frac{1}{r^2} \frac{\partial}{\partial r} \left( \frac{1}{3} n_e \kappa_{\text{Sp}} r^2 \frac{\partial T}{\partial r} \right) \right]^{-1} \quad (50)$$

one can expect in the presence of a tangled magnetic field (i.e.  $f = 1/3$  — e.g. see Gruzinov 2002). Heating via thermal conduction is everywhere unimportant relative to radiative cooling and (by construction) parallel viscous heating. Also note that  $t_{i-e,eq} \lesssim 1$  Myr everywhere in the cluster core, so that the assumption of equal ion and electron temperatures is well justified.

These conclusions are by no means unique to A1835. To demonstrate this point, we plot in Fig. 4b the Spitzer conduction suppression factor  $f$  required for thermal conduction to balance radiative cooling as a function of radius for several different clusters.<sup>9</sup> Only suppression factors  $f \lesssim 1/3$  are expected in the presence of

a tangled magnetic field. None of these clusters can be in thermal balance between thermal conduction and radiative cooling.

## 4 DISCUSSION

In this paper, we have introduced a model for regulating cooling in cluster cores in which turbulence, magnetic fields and plasma physics all play crucial roles. Our findings are fundamentally based on an appreciation that, whatever the source of viscosity in the ICM, it is certainly not hydrodynamic. Instead, the viscosity is set by the microscale plasma-physical processes that are inevitable in a weakly collisional, magnetised environment such as the ICM. Working under the expectation that microscale plasma instabilities pin the pressure anisotropy at its marginally stable value, we derive an expression for the heating rate due to parallel viscous dissipation of turbulent motions. For typical conditions in a variety of cluster cores, this rate is of the right magnitude to balance radiative cooling. Moreover, we have shown that this source of heating is thermally stable. Put simply, the viscosity of the ICM is a dynamic quantity that responds to local changes in temperature, density and magnetic field strength in such a way as to prevent runaway heating or cooling. This is due to the steep increase in the ion-ion collision frequency as the temperature decreases and the density increases. A basic qualitative outline of how this occurs is given in Figure 5. If true, what we have conjectured constitutes a physical mechanism that allows clusters to develop stable non-isothermal temperature profiles and avoid a cooling catastrophe — an outcome that has remained elusive in models involving balancing the cooling by thermal conduction.

Our theory does *not* predict the specific shape of the density and temperature profiles. The most reliable, as well as readily observable, predictions that follow from our theory concern the magnetic field strength. For typical electron densities and temperatures, the resulting magnetic field strengths are  $\sim 1 - 10 \mu\text{G}$ , well within current observational constraints. For the specific clusters discussed here (Hydra A, A1835, A2199, A2382, A2255, Coma), a balance between parallel viscous heating and radiative cooling results in field strengths and profiles that are quite reasonable and in good agreement with current observational estimates where available. It

<sup>9</sup> For the line plots in the figures, we have used analytic fits to the observed electron density and temperature profiles. One advantage is that this ensures smooth gradients for computing the conductive heating rates. The profiles for A478 and A1795 were taken from Dennis & Chandran (2005), the profiles for M87 were taken from Ghizzardi et al. (2004) and the profiles for Virgo were taken from Ghizzardi et al. (2004) and Pope et al. (2006). For A1835 (Sanders et al. 2009) and Hydra A (David et al. 2001), the electron number density was fit using Equation (40) with  $\beta = 0.89$ ,  $r_c = 32.48$  kpc and  $n_0 = 0.115 \text{ cm}^{-3}$  (for A1835) and  $\beta = 0.59$ ,  $r_c = 10.9$  kpc and  $n_0 = 0.0669 \text{ cm}^{-3}$  (for Hydra A). Their temperature profiles were fit using equation (22) of Dennis & Chandran (2005) with  $T_0 = 9.55$  keV,  $T_1 = 7.39$  keV,  $r_{ct} = 33.35$  kpc and  $\delta = 0.62$  (for A1835) and  $T_0 = 3.95$  keV,  $T_1 = 0.856$  keV,  $r_{ct} = 30.60$  kpc and  $\delta = 0.48$  (for Hydra A).

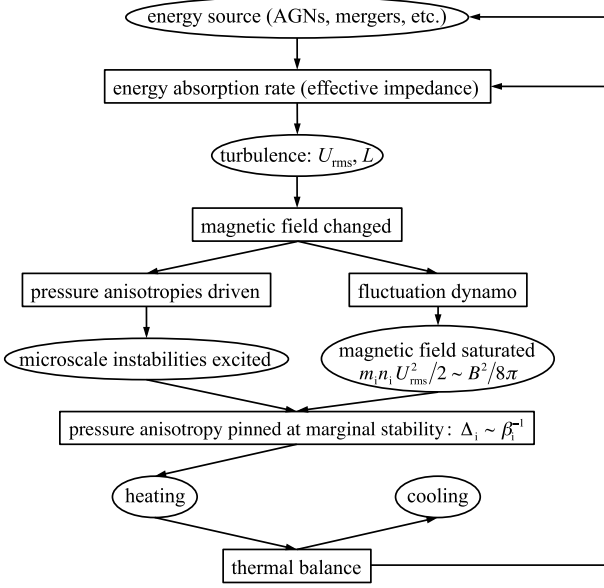


**Figure 5.** Qualitative outline of the processes responsible for thermal balance between parallel viscous heating and radiative cooling. Energy sources (AGNs, mergers, etc.) inject energy into the ICM, some or all of which (depending on the effective impedance of the ICM) is absorbed by the plasma and converted into turbulence. This changes the magnetic field strength, giving rise to both a fluctuation dynamo and pressure anisotropies. The fluctuation dynamo presumably saturates in equipartition between the turbulent magnetic and kinetic energies. The pressure anisotropies excite microscale instabilities, whose effect is to pin the pressure anisotropy at marginal stability. The pressure anisotropy determines the viscous stress and therefore the heating rate. This heating balances radiative cooling, giving rise to a stable thermal equilibrium that is maintained by energy injection by self-regulated sources (such as AGNs) and/or self-regulated energy absorption by the turbulence.

would be interesting to test our model further via analysis of Faraday rotation maps.

Another prediction is the manner in which the magnetic field strength  $B$  depends on electron density  $n_e$  and temperature  $T$  (eq. 29):

$$B \propto n_e^{1/2} T^{3/4} \quad (\text{for cool-core clusters}). \quad (51)$$

In cool-core clusters, this suggests that the oft-employed assumption of an exclusive relationship between  $B$  and  $n_e$  should be relaxed. It is encouraging that, in isothermal clusters, the implied scaling

$$B \propto n_e^{1/2} \quad (\text{for isothermal clusters}) \quad (52)$$

has already been observationally inferred to hold in A2382 (Guidetti et al. 2008), Coma (Bonafede et al. 2010) and A665 (Vacca et al. 2010). A caveat here is that a local heating-cooling balance in such clusters may take very long to establish and so should be treated as a conjecture. A key test of whether this conjecture is reasonable would be to determine whether Equation (52) is satisfied systematically in a large sample of isothermal clusters.

There are several peripheral consequences of our predictions that warrant further discussion. First, the relatively large magnetic field strengths inferred from observed rotation measures and predicted by a balance between parallel viscous heating and radiative cooling are stable or at least marginally stable to the HBI. The stability criterion for the HBI (Quataert 2008) may be written as a

lower-bound on the magnetic field strength:

$$B \gtrsim 3 \left( \frac{g}{10^{-8} \text{ cm s}^{-2}} \right)^{1/2} \left( \frac{n_e}{0.1 \text{ cm}^{-3}} \right)^{1/2} \times \left( \frac{r}{100 \text{ kpc}} \right)^{1/2} \left( \frac{d \ln T / d \ln r}{0.1} \right)^{1/2} \mu\text{G}. \quad (53)$$

Even under the favourable conditions we have chosen for the electron density  $n_e$ , the radial distance from the cluster centre  $r$  and the temperature slope  $d \ln T / d \ln r$ , the magnetic fields predicted in this paper exceed the stability limit (53). Indeed, Bogdanović et al. (2009, § 3.3) and Parrish, Quataert & Sharma (2009a, § 5.7) found that simulated clusters with magnetic field strengths  $B \sim 3 \mu\text{G}$  demonstrated a delayed cooling catastrophe due to the stabilisation of HBI modes by magnetic tension. By contrast, the rms magnetic field strength used in the Parrish, Quataert & Sharma (2009b) simulation, where a combination of turbulent stirring and HBI-governed thermal conduction gave a cool core in long-term thermal balance, was  $10^{-9} \text{ G}$ . More observational estimates of magnetic field strengths in a variety of clusters would be invaluable.

Second, the same process that is responsible for stably heating the ICM in our model may also influence the turbulent diffusion of metals throughout the cores of galactic clusters. That our values for the turbulent diffusion coefficient  $\kappa_{\text{turb}}$  are comparable to those inferred in a variety of clusters is encouraging. However, Rebusco et al. (2005) found that diffusion coefficients that increase with radius (as ours does) imply abundance profiles that are too centrally peaked compared to those observed. It is therefore worth investigating the diffusion of metals using our predicted scaling  $\kappa_{\text{turb}} \propto n_e^{-1} T^{5/2}$ .

Third, turbulent heat diffusion may become dominant relative to collisional electron heat conduction if the Spitzer conductivity suppression factor  $f \lesssim 0.03$  (see eqns 36 and 47). However, for typical density and temperature profiles of cool-core clusters, neither form of heat diffusion seems to be important relative to parallel viscous heating (see Section 3.6).

It is prudent to repeat here our assumptions and their limitations:

(i) We have implicitly assumed that there is enough turbulent energy so that, once thermalised via parallel viscous heating, it can offset cooling. This requires either the source of the turbulent energy or the amount of energy actually accepted by the plasma and converted into turbulent motions to be self-regulating and have some knowledge of the cooling rate.

AGNs are a natural candidate for providing a self-regulating source of energy input, whether the stirring is due to AGN-driven jets, bubbles, weak shocks/sound waves, gravitational modes, and/or cosmic-ray–buoyancy instabilities (see references in footnote 3). Observationally, a large majority of cool-core clusters harbour radio sources at their centres (Burns 1990), and the AGN energy output inferred from radio-emitting plasma outflows and cavities is often similar to the X-ray cooling rate of the central gas (Fabian et al. 2000; Bîrzan et al. 2004; Dunn & Fabian 2006; McNamara & Nulsen 2007; Forman et al. 2007).

However, it may not be necessary for the energy source to be self-regulating. Not all of the power provided by the external driving has to be thermalised via turbulence, as the turbulence may have an effective ‘impedance’ and only accept the amount of power that can be viscously dissipated without triggering the microinstabilities. Indeed, there seems to be no dearth of turbulent power (e.g. Churazov et al. 2004). The fact that some of the turbulent power can be thermalised via parallel viscous dissipation in a thermally-

stable way provides an attractive alternative to other heating models that suffer from stability issues. Further work on the excitation and replenishment of turbulence in a weakly collisional ICM is clearly needed.

(ii) The heating is assumed to be all due to parallel collisional viscosity. In principle, energy could cascade through the parallel viscous scale and onwards to collisionless scales via Alfvénic turbulence and then heat the plasma via microphysical dissipation at the ion and electron Larmor scales (Schekochihin et al. 2009). This possibility has been ignored here.

(iii) The predicted outer-scale turbulent velocity, obtained by assuming approximate equipartition between kinetic and magnetic energies, is probably a lower limit on the actual turbulent velocity since  $U_{\text{rms}}$  is unlikely to be smaller than the Alfvén speed. Unfortunately, a more exact estimate of  $U_{\text{rms}}$  would require a detailed understanding of turbulent dynamo saturation in the ICM, far beyond the scope of the present work.

(iv) Our estimate of the turbulent outer scale is perhaps the most uncertain of our predictions, as it depends on the rate of transfer of energy from the external driving sources into the turbulence. This encodes what we have referred to as the effective ‘impedance’ of the turbulence, the detailed physics of which is poorly understood.

All these issues clearly require further theoretical work. However, the fact that our predictions are not too far from current observational estimates or plausible expectations lends us hope that these concerns might be of secondary importance.

While the exact numbers predicted in this paper should be taken with a grain of salt, one cannot help being encouraged by the fact that they seem to be quite reasonable without any fine-tuning of adjustable prefactors. The basic premise that the saturation of microscale plasma instabilities endows the ICM with a thermally stable source of viscous heating seems robust. If our predictions are confirmed, they would constitute strong evidence that microphysical plasma processes play a decisive role in setting the large-scale structure and evolution of galaxy clusters.

## ACKNOWLEDGMENTS

It is a pleasure to thank Steve Balbus, Torsten Enßlin, Andy Fabian, Petr Kuchar, Ian Parrish, Eliot Quataert, Mark Rosin and Prateek Sharma for useful discussions, as well as Helen Russell for graciously providing observational data for several clusters. We also thank Annalisa Bonafede for kindly making the data used in Fig. 3 available to us. This work was supported by the STFC.

## REFERENCES

- Arnaud M., Aghanim N., Gastaud R., et al., 2001, *A&A*, 365, L67  
 Balbus S. A., 2000, *ApJ*, 534, 420  
 Balbus S. A., 2001, *ApJ*, 562, 909  
 Balbus S. A., Reynolds C. S., 2008, *ApJ*, 681, 65  
 Bale S. D., Kasper J. C., Howes G. G., Quataert E., Salem C., Sundkvist D., 2009, *Phys. Rev. Lett.*, 103, 211101  
 Bertschinger E., Meiksen A., 1986, *ApJ*, 306, L1  
 Binney J., 2004, in T. H. Reiprich, J. C. Kempner, N. Soker, eds, *The Riddle of Cooling Flows in Galaxies and Cluster of Galaxies*. <http://www.astro.virginia.edu/coolflow/proc.php>, p. 233  
 Binney J., 2005, *Phil. Trans. R. Soc. London, A*, 363, 739  
 Binney J., Cowie L. L., 1981, *ApJ*, 247, 464  
 Binney J., Tabor G., 1995, *MNRAS*, 276, 663  
 Bîrzan L., Rafferty D. A., McNamara B. R., Wise M. W., Nulsen P. E. J., 2004, *ApJ*, 607, 800  
 Bogdanović T., Reynolds C. S., Balbus S. A., Parrish I. J., 2009, *ApJ*, 704, 211  
 Bonafede A., Feretti L., Murgia M., Govoni F., Giovannini G., Dallacasa D., Dolag K., Taylor G. B., 2010, *arXiv:1002.0594*  
 Braginskii S. I., 1965, *Rev. Plasma Phys.*, 1, 205  
 Bregman J. N., David L. P., 1988, *ApJ*, 326, 639  
 Brighenti F., Mathews W. G., 2003, *ApJ*, 587, 580  
 Brüggén M., 2003, *ApJ*, 593, 700  
 Brüggén M., Kaiser C. R., 2002, *Nature*, 418, 301  
 Brüggén M., Scannapieco E., 2009, *MNRAS*, 398, 548  
 Brüggén M., Ruszkowski M., Hallman E., 2005, *ApJ*, 630, 740  
 Burns J. O., 1990, *AJ*, 99, 14  
 Califano F., Hellinger P., Kuznetsov E., Passot T., Sulem P. L., Trávníček P. M., 2008, *J. Geophys. Res.*, 113, A08219  
 Carilli C. L., Taylor G. B., 2002, *ARA&A*, 40, 319  
 Cavaliere A., Fusco-Femiano R., 1976, *A&A*, 49, 137  
 Chandran B. D. G., 2004, *ApJ*, 616, 169  
 Chandran B. D. G., 2005, *ApJ*, 632, 809  
 Chandran B. D. G., Cowley S. C., 1998, *Phys. Rev. Lett.*, 80, 3077  
 Chandran B. D. G., Rasera Y., 2007, *ApJ*, 671, 1413  
 Chandran B. D. G., Cowley S. C., Ivanushkina M., Sydora R., 1999, *ApJ*, 525, 638  
 Cho J., Lazarian A., Honein A., Knaepen B., Kassinos S., Moin P., 2003, *ApJ*, 589, L77  
 Churazov E., Forman W., Jones C., Sunyaev R., Böhringer H., 2004, *MNRAS*, 347, 29  
 Ciotti L., Ostriker J. P., 2001, *ApJ*, 551, 131  
 Ciotti L., Ostriker J. P., 2007, *ApJ*, 665, 1038  
 Conroy C., Ostriker J. P., 2008, *ApJ*, 681, 151  
 Cowie L. L., Binney J., 1977, *ApJ*, 215, 723  
 David L. P., Nulsen P. E. J., 2008, *ApJ*, 689, 837  
 David L. P., Nulsen P. E. J., McNamara B. R., Forman W., Jones C., Ponman T., Robertson B., Wise M., 2001, *ApJ*, 557, 546  
 Davis D. S., White III. R. E., 1998, *ApJ*, 492, 57  
 Deiss B. M., Just A., 1996, *A&A*, 305, 407  
 Dekel A., Birnboim Y., 2008, *MNRAS*, 383, 119  
 Dennis T. J., Chandran B. D. G., 2005, *ApJ*, 622, 205  
 Dolag K., Schindler S., Govoni F., Feretti L., 2001, *A&A*, 378, 777  
 Donahue M., Horner D. J., Cavagnolo K. W., Voit G. M., 2006, *ApJ*, 643, 730  
 Dunn R. J. H., Fabian A. C., 2006, *MNRAS*, 373, 959  
 Edge A. C., Stewart G. C., Fabian A. C., 1992, *MNRAS*, 258, 177  
 El-Zant A. A., Kim W.-T., Kamionkowski M., 2004, *MNRAS*, 354, 169  
 Enßlin T. A., Vogt C., 2006, *A&A*, 453, 447  
 Fabian A. C., 1994, *ARA&A*, 32, 277  
 Fabian A. C., Nulsen P. E. J., 1977, *MNRAS*, 180, 479  
 Fabian A. C., Sanders J. S., Ettori S., et al., 2000, *MNRAS*, 318, L65  
 Fabian A. C., Voigt L. M., Morris R. G., 2002, *MNRAS*, 335, L71  
 Fabian A. C., Reynolds C. S., Taylor G. B., Dunn R. J. H., 2005, *MNRAS*, 363, 891  
 Feretti L., Böhringer H., Giovannini G., Neumann D., 1997, *A&A*, 317, 432  
 Field G. B., 1965, *ApJ*, 142, 531  
 Forman W., Jones C., Churazov E., et al., 2007, *ApJ*, 665, 1057  
 Fujita Y., 2005, *ApJ*, 631, L17  
 Fujita Y., Suzuki T. K., 2005, *ApJ*, 630, L1  
 Gaetz T. J., 1989, *ApJ*, 345, 666

- Ghizzardi S., Molendi S., Pizzolato F., De Grandi S., 2004, *ApJ*, 609, 638
- Govoni F., Murgia M., Feretti L., Giovannini G., Dolag K., Taylor G. B., 2006, *A&A*, 460, 425
- Graham J., Fabian A. C., Sanders J. S., Morris R. G., 2006, *MNRAS*, 368, 1369
- Gruzinov A., 2002, arXiv:0203031
- Guidetti D., Murgia M., Govoni F., Parma P., Gregorini L., de Ruiter H. R., Cameron R. A., Fanti R., 2008, *A&A*, 483, 699
- Guo F., Oh S. P., 2008, *MNRAS*, 384, 251
- Guo F., Oh S. P., Ruszkowski M., 2008, *ApJ*, 688, 859
- Haugen N. E., Brandenburg A., Dobler W., 2004, *Phys. Rev. E*, 70, 6308
- Hellinger P., Trávníček P., Kasper J. C., Lazarus A. J., 2006, *Geophys. Res. Lett.*, 33, L09101
- Hoeft M., Brüggen M., 2004, *ApJ*, 617, 896
- Iapichino L., Niemeyer J. C., 2008, *MNRAS*, 388, 1089
- Istomin Ya. N., Pokhotelov O. A., Balikhin M. A., 2009, *Phys. Plasmas*, 16, 062905
- Johnstone R. M., Allen S. W., Fabian A. C., Sanders J. S., 2002, *MNRAS*, 336, 299
- Just A., Deiss B. M., Kegel W. H., Böhringer H., Morfill G. E., 1990, *ApJ*, 354, 400
- Kaastra J. S., Tamura T., Peterson J. R., et al., 2004, *A&A*, 413, 415
- Kaiser C. R., Binney J., 2003, *MNRAS*, 338, 837
- Kasper J. C., Lazarus A. J., Gary S. P., 2002, *Geophys. Res. Lett.*, 29, 1839
- Kim W.-T., Narayan R., 2003a, *ApJ*, 596, L139
- Kim W.-T., Narayan R., 2003b, *ApJ*, 596, 889
- Kim W.-T., El-Zant A. A., Kamionkowski M., 2005, *ApJ*, 632, 157
- Kuchar P., Enßlin T., 2009, arXiv:0912.3930
- Lea S. M., De Young D. S., 1976, *ApJ*, 210, 647
- Loewenstein M., Fabian A. C., 1990, *MNRAS*, 242, 120
- Lyutikov M., 2007, *ApJ*, 668, L1
- McCarthy I. G., Babul A., Bower R. G., Balogh M. L., 2008, *MNRAS*, 386, 1309
- McNamara B. R., Nulsen P. E. J., 2007, *ARA&A*, 45, 117
- Markevitch M., Mazzotta P., Vikhlinin A., et al., 2003, *ApJ*, 586, L19
- Mathews W. G., Bregman J. N., 1978, *ApJ*, 224, 308
- Mathews W. G., Faltenbacher A., Brighenti F., 2006, *ApJ*, 638, 659
- Matteini L., Landi S., Hellinger P., Velli M., 2006, *J. Geophys. Res.*, 111, A10101
- Matteini L., Landi S., Hellinger P., Pantellini F., Maksimovic M., Velli M., Goldstein B. E., Marsch E., 2007, *Geophys. Res. Lett.*, 34, L20105
- Miller L., 1986, *MNRAS*, 220, 713
- Murgia M., Govoni F., Feretti L., Giovannini G., Dallacasa D., Fanti R., Taylor G. B., Dolag K., 2004, *A&A*, 424, 429
- Murgia M., Govoni F., Markevitch M., Feretti L., Giovannini G., Taylor G. B., Carretti E., 2009, *A&A*, 499, 679
- Narayan R., Medvedev M. V., 2001, *ApJ*, 562, L129
- Norman M. L., Bryan G. L., 1999, *LNP*, 530, 106
- Nusser A., Silk J., Babul A., 2006, *MNRAS*, 373, 739
- Omma H., Binney J., 2004, *MNRAS*, 350, L13
- Parrish I. J., Quataert E., 2008, *ApJ*, 677, L9
- Parrish I. J., Quataert E., Sharma P., 2009a, *ApJ*, 703, 96
- Parrish I. J., Quataert E., Sharma P., 2009b, arXiv:0912.1851
- Peres C. B., Fabian A. C., Edge A. C., Allen S. W., Johnstone R. M., White D. A., 1998, *MNRAS*, 298, 416
- Peterson J. R., Fabian A. C., 2006, *Phys. Rep.*, 427, 1
- Peterson J. R., Paerels F. B. S., Kaastra J. S., et al., 2001, *A&A*, 365, L104
- Peterson J. R., Kahn S. M., Paerels F. B. S., Kaastra J. S., Tamura T., Bleeker J. A. M., Ferrigno C., Jernigan J. G., 2003, *ApJ*, 590, 207
- Piffaretti R., Jetzer Ph., Kaastra J. S., Tamura T., 2005, *A&A*, 433, 101
- Pistinner S., Shaviv G., 1996, *ApJ*, 459, 147
- Pollack L. K., Taylor G. B., & Allen S. W., 2005, *MNRAS*, 359, 1229
- Pope E. C. D., Pavlovski G., Kaiser C. R., Fangohr H., 2006, *MNRAS*, 367, 1121
- Quataert E., 2008, *ApJ*, 673, 758
- Quest K. B., Shapiro V. D., 1996, *J. Geophys. Res.*, 101, 24457
- Rebusco P., Churazov E., Böhringer H., Forman W., 2005, *MNRAS*, 359, 1041
- Rebusco P., Churazov E., Böhringer H., Forman W., 2006, *MNRAS*, 372, 1840
- Rebusco P., Churazov E., Sunyaev R., Böhringer H., Forman W., 2008, *MNRAS*, 384, 1511
- Raphaeli Y., Salpeter E. E., 1980, *ApJ*, 240, 20
- Ricker P. M., Sarazin C. L., 2001, *ApJ*, 561, 621
- Rosin M. S., Schekochihin A. A., Rincon F., Cowley S. C., 2010, *MNRAS*, submitted (arXiv:1002.4017)
- Rosner R., Tucker W. H., 1989, *ApJ*, 338, 761
- Ruszkowski M., Begelman M. C., 2002, *ApJ*, 581, 223
- Ruszkowski M., Oh S. P., 2009, arXiv:0911.5198
- Ruszkowski M., Brüggen M., Begelman M. C., 2004a, *ApJ*, 611, 158
- Ruszkowski M., Brüggen M., Begelman M. C., 2004b, *ApJ*, 615, 675
- Sakelliou I., Ponman T. J., 2006, *MNRAS*, 367, 1409
- Sanders J. S., Fabian A. C., Smith R. K., Peterson J. R., 2010, 402, L11
- Sanderson A. J. R., Ponman T. J., O' Sullivan E., 2006, *MNRAS*, 372, 1496
- Sarazin C. L., 1986, *Rev. Mod. Phys.*, 58, 1
- Sarazin C. L., 1988, *X-Ray Emissions from Clusters of Galaxies*. Cambridge Univ. Press, Cambridge
- Schekochihin A. A., Cowley S. C., 2006, *Physics of Plasmas*, 13, 056501
- Schekochihin A. A., Cowley S. C., 2007, in Molokov S., Moreau R., Moffrat H. K., eds, *Magnetohydrodynamics: Historical Evolution and Trends*. Springer, Dordrecht, p. 85
- Schekochihin A. A., Cowley S. C., Taylor S. F., Maron J. L., McWilliams J. C., 2004, *ApJ*, 612, 276
- Schekochihin A. A., Cowley S. C., Kulsrud R. M., Hammett G. W., Sharma P., 2005, *ApJ*, 629, 139
- Schekochihin A. A., Cowley S. C., Kulsrud R. M., Rosin M. S., Heinemann T., 2008, *Phys. Rev. Lett.*, 100, 081301
- Schekochihin A. A., Cowley S. C., Dorland W., Hammett G. W., Howes G. G., Quataert E., Tatsuno T., 2009, *ApJS*, 182, 310
- Schekochihin A. A., Cowley S. C., Rincon F., Rosin M. S., 2010, *MNRAS*, in press (arXiv:0912.1359)
- Schipper L., 1974, *MNRAS*, 168, 21
- Schuecker P., Finoguenov A., Miniati F., Böhringer H., Briel U. G., 2004, *A&A*, 426, 387
- Shapiro V. D., Shevchenko V. I., 1964, *Sov. Phys. JETP*, 18, 1109
- Sharma P., Hammett G. W., Quataert E., Stone J. M., 2006, *ApJ*,

- 637, 952
- Sharma P., Quataert E., Hammett G., Stone J. M., 2007, *ApJ*, 667, 714
- Sharma P., Chandran B. D. G., Quataert E., Parrish I. J., 2009, arXiv:0909.0270
- Sijacki D., Pfrommer C., Springel V., Enßlin T. A., 2008, *MNRAS*, 387, 1403
- Soker N., 2003, *MNRAS*, 342, 463
- Spitzer L. Jr., 1962, *Physics of Fully Ionized Gases*. Wiley Interscience, New York, NY
- Subramanian K., Shukurov A., Haugen N. E. L., 2006, *MNRAS*, 366, 1437
- Sunyaev R. A., Norman M. L., Bryan G. L., 2003, *Astron. Lett.*, 29, 783
- Sutherland R. S., Dopita M. A., 1993, *ApJS*, 88, 253
- Tao L., 1995, *MNRAS*, 275, 965
- Tozzi P., Norman C., 2001, *ApJ*, 546, 63
- Tribble P. C., 1989, *MNRAS*, 238, 1247
- Tucker W. H., Rosner R., 1983, *ApJ*, 267, 547
- Vacca V., Murgia M., Govoni F., Feretti L., Giovannini G., Orrù E., Bonafede A., 2010, arXiv:1001.1058
- Vikhlinin A., Markevitch M., Murray S. S., Jones C., Forman W., Van Speybroeck L., 2005, *ApJ*, 628, 655
- Vikhlinin A., Kravtsov A., Forman W., Jones C., Markevitch M., Murray S. S., & Van Speybroeck L., 2006, *ApJ*, 640, 691
- Voigt L. M., Fabian A. C., 2004, *MNRAS*, 347, 1130
- Voigt L. M., Schmidt R. W., Fabian A. C., Allen S. W., Johnstone R. M., 2002, *MNRAS*, 335, L7
- Voit G. M., Donahue M., 2005, *ApJ*, 634, 955
- Vogt C., Enßlin T. A., 2003, *A&A*, 412, 373
- Vogt C., Enßlin T. A., 2005, *A&A*, 434, 67
- Zakamska N. L., Narayan R., 2003, *ApJ*, 582, 162

This paper has been typeset from a  $\text{\LaTeX}$  file prepared by the author.